ESTIMATION OF SONIC FATIGUE BY
REDUCED-ORDER FINITE ELEMENT BASED ANALYSES

Stephen A. Rizzi
NASA Langley Research Center, Structural Acoustics Branch
Hampton, Virginia 23681-2199, USA.   Email: stephen.a.rizzi@nasa.gov

Adam Przekop
National Institute of Aerospace
Hampton, Virginia 23666-6147, USA.   Email: adam@nianet.org

ABSTRACT

A computationally efficient, reduced-order method is presented for prediction of sonic fatigue of structures exhibiting geometrically nonlinear response. A procedure to determine the nonlinear modal stiffness using commercial finite element codes allows the coupled nonlinear equations of motion in physical degrees of freedom to be transformed to a smaller coupled system of equations in modal coordinates. The nonlinear modal system is first solved using a computationally light equivalent linearization solution to determine if the structure responds to the applied loading in a nonlinear fashion. If so, a higher fidelity numerical simulation in modal coordinates is undertaken to more accurately determine the nonlinear response. Comparisons of displacement and stress response obtained from the reduced-order analyses are made with results obtained from numerical simulation in physical degrees-of-freedom. Fatigue life predictions from nonlinear modal and physical simulations are made using the rainflow cycle counting method in a linear cumulative damage analysis. Results computed for a simple beam structure under a random acoustic loading demonstrate the effectiveness of the approach and compare favorably with results obtained from the solution in physical degrees-of-freedom.

INTRODUCTION

Sonic fatigue is an on-going concern for high-speed aircraft and reusable launch vehicle structures because of their exposure to high vibroacoustic environments. Such loadings often induce geometrically nonlinear response in thin-walled structures, thereby requiring a nonlinear random response analysis. Further, a finite-element-based approach is usually required due to the geometrical complexity of these structures. Sonic fatigue prediction by solution in physical degrees-of-freedom (DoFs) is not attractive because of the computational burden associated with a large system size and long simulation time [1] required to obtain accurate fatigue estimates. Therefore, reduction of the system is sought to make the solution more tractable.

Within the context of a finite element formulation, several approaches have been developed to transform the geometrically nonlinear system in physical DoFs to a smaller coupled nonlinear system in modal coordinates. The method employed in this paper indirectly evaluates the nonlinear stiffness [2, 3] to allow implementation using the commercial finite element

1

programs MSC.NASTRAN and ABAQUS. Within those codes, standard solution procedures are used whenever possible, including pre-processing, eigenanalysis to extract modal basis vectors, nonlinear static solutions to determine the nonlinear stiffness, and stress recovery. Once the nonlinear stiffness is determined, the reduced-order coupled system of equations is solved for the modal displacements, which can subsequently be transformed back to physical coordinates and post-processed to obtain stress time histories.

Two solutions procedures are offered. One is a fast, equivalent linearization procedure, which provides useful information about the nonlinear response in an RMS sense. Hence, it is a useful tool for screening the structural response for nonlinear behavior. It was previously found that equivalent linearization could also provide useful fatigue life estimates, but only when the contribution of membrane stress to the total stress was small [4]. The other, more robust procedure, is nonlinear modal simulation and is used to provide accurate displacement and stress time histories when a nonlinear response is indicated. Response results obtained from the reduced-order analyses are compared with those obtained from numerical simulation in physical DoFs. Fatigue estimates are computed from stress time histories using a rainflow cycle counting analysis and linear cumulative damage. Estimates made using nonlinear modal simulation stress time histories are compared with those obtained using results from the simulation in physical DoFs. A simple beam structure is used to illustrate the quality of reduced-order analysis results achievable, while keeping the numerical simulation analysis reasonable.

NONLINEAR MODAL REDUCTION

The equations of motion of the nonlinear system in physical DoFs may be written as

$$M\ddot{X}(t) + C\dot{X}(t) + F_{NL}(X(t)) = F(t) \tag{1}$$

where M and C are the system mass and damping matrices, X is the displacement response vector and F is the force excitation vector, respectively. As written, the nonlinear restoring force F_{NL} is a vector function, which generally includes the linear, quadratic and cubic stiffness terms.

A set of coupled modal equations with reduced DoFs is first obtained by applying the modal coordinate transformation $X = \Phi q$ to Equation (1), where q is the modal displacement response vector. The modal basis matrix Φ is typically formed from the eigenvectors obtained from Equation (1) using only the linear stiffness. Generally, a small set of L basis functions are included giving

$$\tilde{M}\ddot{q}(t) + \tilde{C}\dot{q}(t) + \tilde{F}_{NL}(q_1(t), q_2(t), \ldots, q_L(t)) = \tilde{F}(t) \tag{2}$$

where, for mass-normalized eigenvectors,

$$\tilde{M} = \Phi^T M \Phi = \lceil I \rfloor \qquad \tilde{C} = \Phi^T C \Phi = \lceil 2\zeta_r \omega_r \rfloor \qquad \tilde{F}_{NL} = \Phi^T F_{NL} \qquad \tilde{F} = \Phi^T F \tag{3}$$

and ω_r are the undamped natural frequencies and ζ_r are the viscous damping factors.

Nonlinear modal stiffness evaluation. The direct transformation of Equation (1) to (2) requires knowledge of the system matrices and excitation vector. In the context of a commercial finite element program, the nonlinear restoring force F_{NL} is generally not known. Therefore, an indirect means [2, 3] of evaluating the nonlinear stiffness is applied. The nonlinear modal restoring force may be written in the form

$$\tilde{F}_{NL}(q_1, q_2, \ldots, q_L) = \sum_{j=1}^{L} d_j^r q_j + \sum_{j=1}^{L}\sum_{k=j}^{L} a_{jk}^r q_j q_k + \sum_{j=1}^{L}\sum_{k=j}^{L}\sum_{l=k}^{L} b_{jkl}^r q_j q_k q_l \qquad r = 1, 2, \ldots, L \qquad (4)$$

where d, a, and b are the linear, quadratic nonlinear, and cubic nonlinear modal stiffness coefficients, respectively. This form of $\tilde{F}_{NL}$ reduces the problem of determining the nonlinear stiffness from one in which a large set of simultaneous nonlinear equations must be solved to one involving simple algebraic relations.

The coefficients are obtained through a series of nonlinear static solutions using prescribed static displacement fields X_c in physical coordinates. For coefficients having all the same lower indices, that is, for $[d_j^r]$, $[a_{jj}^r]$, and $[b_{jjj}^r]$ $(j = 1, 2, \ldots, L)$, a set of three displacement fields are prescribed [3]. For example, for $j = 1$, the three displacement fields

$$X_{c1} = +\phi_1 q_1 \qquad X_{c2} = -\phi_1 q_1 \qquad X_{c3} = +\phi_1 \hat{q}_1 \qquad (5)$$

are applied. The modal displacements q and $\hat{q}$ are two different scalar quantities and are specified such that the magnitude of the prescribed physical displacement field X_c is physically meaningful. The corresponding nonlinear restoring force is evaluated using the nonlinear static solution within a commercial finite element program, and is given as

$$\tilde{F}_{NL_1} = \Phi^T F_{NL}(+\phi_1 q_1) = +\left[d_1^r \right] q_1 + \left[a_{11}^r \right] q_1 q_1 + \left[b_{111}^r \right] q_1 q_1 q_1$$

$$\tilde{F}_{NL_2} = \Phi^T F_{NL}(-\phi_1 q_1) = -\left[d_1^r \right] q_1 + \left[a_{11}^r \right] q_1 q_1 - \left[b_{111}^r \right] q_1 q_1 q_1 \qquad (6)$$

$$\tilde{F}_{NL_3} = \Phi^T F_{NL}(+\phi_1 \hat{q}_1) = +\left[d_1^r \right] \hat{q}_1 + \left[a_{11}^r \right] \hat{q}_1 \hat{q}_1 - \left[b_{111}^r \right] \hat{q}_1 \hat{q}_1 \hat{q}_1$$

from which the coefficients $[d_1^r]$, $[a_{11}^r]$ and $[b_{111}^r]$ are obtained. The remaining coefficients $[d_j^r]$, $[a_{jj}^r]$ and $[b_{jjj}^r]$ $(j = 2, 3, \ldots, L)$ are determined in an analogous manner. In this paper, modal displacement values of $q = 7 \times 10^{-5}$ and $\hat{q} = 8.75 \times 10^{-5}$ were used for each occurrence. It has been shown that the stiffness coefficients obtained via this approach are not sensitive to the particular value of modal displacement specified [2, 5].

A similar technique can be employed to determine stiffness coefficients with two unequal lower indices, e.g. $[a_{12}^r]$, $[b_{112}^r]$, and $[b_{122}^r]$. Coefficients of this type appear only if the number of retained eigenvectors is greater than or equal to two ($L \geq 2$). Prescribing the displacement fields

$$X_{c1} = +\phi_1 q_1 + \phi_2 q_2 \qquad X_{c2} = -\phi_1 q_1 - \phi_2 q_2 \qquad X_{c3} = +\phi_1 q_1 - \phi_2 q_2 \qquad (7)$$

results in the following equations

$$\tilde{F}_{NL_1} = \Phi^T F_{NL}(+\phi_1 q_1 + \phi_2 q_2) = +\left[d_1^r\right]q_1 + \left[d_2^r\right]q_2 + \left[a_{11}^r\right]q_1 q_1 + \left[b_{111}^r\right]q_1 q_1 q_1 + \left[a_{22}^r\right]q_2 q_2$$
$$+\left[b_{222}^r\right]q_2 q_2 q_2 + \left[a_{12}^r\right]q_1 q_2 + \left[b_{112}^r\right]q_1 q_1 q_2 + \left[b_{122}^r\right]q_1 q_2 q_2$$

$$\tilde{F}_{NL_2} = \Phi^T F_{NL}(-\phi_1 q_1 - \phi_2 q_2) = -\left[d_1^r\right]q_1 - \left[d_2^r\right]q_2 + \left[a_{11}^r\right]q_1 q_1 - \left[b_{111}^r\right]q_1 q_1 q_1 + \left[a_{22}^r\right]q_2 q_2$$
$$-\left[b_{222}^r\right]q_2 q_2 q_2 + \left[a_{12}^r\right]q_1 q_2 - \left[b_{112}^r\right]q_1 q_1 q_2 - \left[b_{122}^r\right]q_1 q_2 q_2$$

$$\tilde{F}_{NL_3} = \Phi^T F_{NL}(+\phi_1 q_1 - \phi_2 q_2) = +\left[d_1^r\right]q_1 - \left[d_2^r\right]q_2 + \left[a_{11}^r\right]q_1 q_1 + \left[b_{111}^r\right]q_1 q_1 q_1 + \left[a_{22}^r\right]q_2 q_2$$
$$-\left[b_{222}^r\right]q_2 q_2 q_2 - \left[a_{12}^r\right]q_1 q_2 - \left[b_{112}^r\right]q_1 q_1 q_2 + \left[b_{122}^r\right]q_1 q_2 q_2$$

(8)

from which $[a_{12}^r]$, $[b_{112}^r]$, and $[b_{122}^r]$ are determined. All remaining coefficients of the type $[a_{jk}^r]$, $[b_{jjk}^r]$ and $[b_{kkj}^r]$ for $j,k = 1,2,\ldots,L$ are found in this manner.

Finally, for cases when the number of retained eigenvectors if greater than or equal to three ($L \geq 3$), coefficients with three unequal lower indices, e.g. $[b_{123}^r]$, are determined by prescribing the displacement field

$$X_c = +\phi_1 q_1 + \phi_2 q_2 + \phi_3 q_3 \tag{9}$$

The resulting equation

$$\tilde{F}_{NL} = \Phi^T F_{NL}(+\phi_1 q_1 + \phi_2 q_2 + \phi_3 q_3)$$
$$= +\left[d_1^r\right]q_1 + \left[d_2^r\right]q_2 + \left[d_3^r\right]q_3$$
$$+\left[a_{11}^r\right]q_1 q_1 + \left[a_{22}^r\right]q_2 q_2 + \left[a_{33}^r\right]q_3 q_3 + \left[a_{12}^r\right]q_1 q_2 + \left[a_{13}^r\right]q_1 q_3 + \left[a_{23}^r\right]q_2 q_3 \tag{10}$$
$$+\left[b_{111}^r\right]q_1 q_1 q_1 + \left[b_{222}^r\right]q_2 q_2 q_2 + \left[b_{333}^r\right]q_3 q_3 q_3 + \left[b_{112}^r\right]q_1 q_1 q_2 + \left[b_{221}^r\right]q_2 q_2 q_1$$
$$+\left[b_{113}^r\right]q_1 q_1 q_3 + \left[b_{331}^r\right]q_3 q_3 q_1 + \left[b_{223}^r\right]q_2 q_2 q_3 + \left[b_{332}^r\right]q_3 q_3 q_2 + \left[b_{123}^r\right]q_1 q_2 q_3$$

contains one column of unknown coefficients $[b_{123}^r]$. All remaining coefficients of type $[b_{jkl}^r]$ ($j \neq k \neq l$) are found in this manner.

The number of nonlinear static solutions required depends on the number of modes selected (L) and may be expressed as:

$$\text{Number of Solutions} = 3\binom{L}{1} + 3\binom{L}{2} + \binom{L}{3} \tag{11}$$

where

$$\binom{L}{n} = \frac{L!}{n!(L-n)!} \tag{12}$$

is the number of order-independent combinations of n modes from the L selected modes. For example, if $L = 12$, the number of nonlinear static solutions required is 454. The stiffness evaluation procedure is performed independent of loading. Therefore, the procedure need only be performed once prior to the solution of Equation (2). The particular selection of modal basis, however, will be influenced by factors including the structural geometry, material properties, and loading distribution. Recent work by the authors investigated basis selection for flat [5] and curved structures [6].

Implementation. The nonlinear stiffness evaluation method, and numerical integration and equivalent linearization solutions to follow, are embodied in the program RANSTEP, for "*R*educed order *A*nalysis using a *N*onlinear *ST*iffness *E*valuation *P*rocedure." RANSTEP has been implemented for use with two commercial finite element programs; MSC.NASTRAN version 2005 and ABAQUS version 6.5.

To obtain the modal basis matrix $\mathbf{\Phi}$ for the coordinate transformation $X = \mathbf{\Phi}q$, the NASTRAN implementation uses a direct matrix abstraction program (DMAP) to write mass-normalized eigenvectors from the standard normal modes analysis (solution 103). The ABAQUS implementation uses a PYTHON script to access mass-normalized eigenvectors from the output database created using the *FREQUENCY analysis in ABAQUS Standard.

For both implementations, an external FORTRAN program forms the set of prescribed displacement fields, as per Equations (5), (7) and (9). Since the displacement fields are formed outside of the finite element program, other basis functions may be utilized, e.g. experimentally determined, however these are not considered in the present work. A static nonlinear analysis follows to determine the corresponding nonlinear restoring forces. In the NASTRAN implementation, a DMAP code is used to modify the standard nonlinear static analysis (solution 106) to allow specification of the displacement fields and output of the nonlinear restoring forces. In the ABAQUS implementation, a PYTHON script extracts the forces from the output database created using the *STATIC analysis (with geometric nonlinearity enabled) in ABAQUS Standard. The nonlinear stiffness coefficients are determined from Equations (6), (8) and (10) in an external FORTRAN code using the nonlinear forces from the above analyses.

Nonlinear stiffness validation. Validation of the nonlinear modal stiffness formulation and implementation was performed using an aluminum beam under a uniformly distributed pressure loading. The beam measured 18-in. x 1-in. x 0.09-in (*l* x *w* x *h*) and was fully clamped at both ends. The following material properties were used:

$$E = 10.6 \times 10^6 \, psi, \qquad G = 4.0 \times 10^6 \, psi, \qquad \rho = 2.588 \times 10^{-4} \, \frac{lb_f - s^2}{in^4}$$

Displacements and stresses obtained from nonlinear modal solutions using different modal bases were compared with those obtained directly from a full nonlinear analysis in physical DoFs. A static loading was selected to eliminate any dynamic effects associated with the modal mass and damping. Hence, only the modal stiffness coefficients dictate the accuracy of the solution for a particular basis. While it is possible to set the modal accelerations and velocities to zero in Equation (2) and solve for the modal displacements via Newton-Raphson (as per [2]), the more direct approach utilized here applies the load quasi-statically and numerically integrates Equation (2) to obtain the modal displacements. The modal numerical integration procedure used is discussed in the next section. The modal displacements are transformed to physical coordinates and stresses are obtained through post-processing, in a procedure also discussed in the next section.

The quasi-static pressure loading was applied to the beam with a loading time history ramped from zero magnitude at time zero to its maximum level at 1.6384s. The response was obtained after an additional 0.5s at the maximum loading level to allow for the decay of any transient behavior.

For the reduced order analysis, the beam was modeled in MSC.NASTRAN using 144 CBEAM elements. The analysis in physical DoFs was performed using the ABAQUS explicit solution. The double precision explicit integration scheme with an adaptive time

integration step (referred to as "element by element" in ABAQUS) was utilized for the quasi-static and subsequent dynamic analyses. The ABAQUS model consisted of 144 B21 elements. Differences between the ABAQUS and MSC.NASTRAN element formulations were previously found to be negligible [5].

It was previously shown that a basis consisting of a single mode could exactly reconstruct the displacement when the applied loading distribution was identical to the mode shape [2]. For other distributions, bases consisting of a number of modes are required to obtain an accurate solution. For the present analysis, two modal bases were considered. The first basis consisted of a combination of uncoupled low-frequency bending modes and high-frequency membrane modes. The inclusion of both bending and membrane modes in the basis captures the effect of nonlinear bending-membrane coupling. In particular, the basis considered was comprised of the first six symmetric bending modes and the first six anti-symmetric membrane modes. A second modal basis consisting of only the first six bending modes was also considered. This basis is consistent with subsequent linear and equivalent linear analyses, for which there is no nonlinear bending-membrane coupling. As such, the basis is not capable of predicting the membrane displacement response under a transverse loading.

Shown in Figure 1 is the transverse displacement response for the two modal bases. The displacement results obtained using both bases are comparable to each other and compare well with the physical DoF solution As expected, only the basis consisting of bending and membrane modes compares well with the physical DoF solution for the membrane displacement, as shown in Figure 2. The stress response is shown in Figure 3 and Figure 4 for the bending and membrane components, respectively. The fact that there are several points along the beam where membrane stress results from the bending only basis agrees with the physical DoFs solution highlights the need to consider a number of spatial locations in assessing the accuracy of the modal basis.
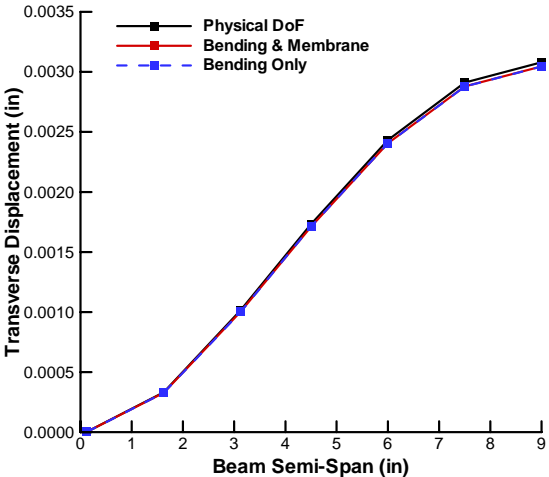

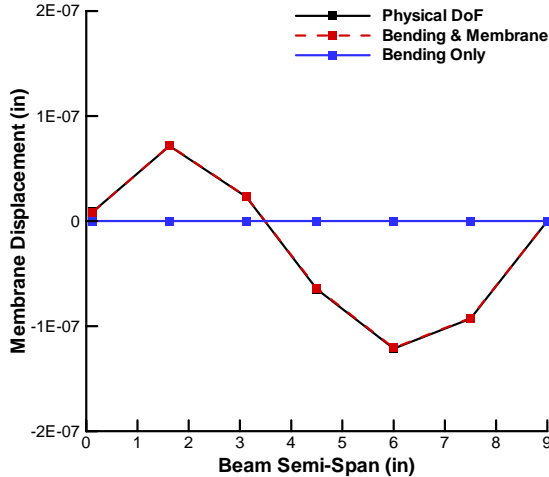*Figure 1: Quasi-static transverse displacement along beam under 0.0576 psi pressure load.*

Figure 2: Quasi-static membrane displacement along beam under 0.0576 psi pressure load.
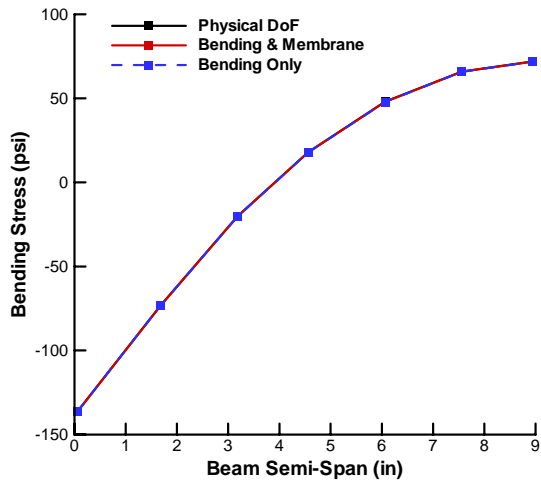
6

Figure 3: Quasi-static bending stress along beam under 0.0576 psi pressure load.
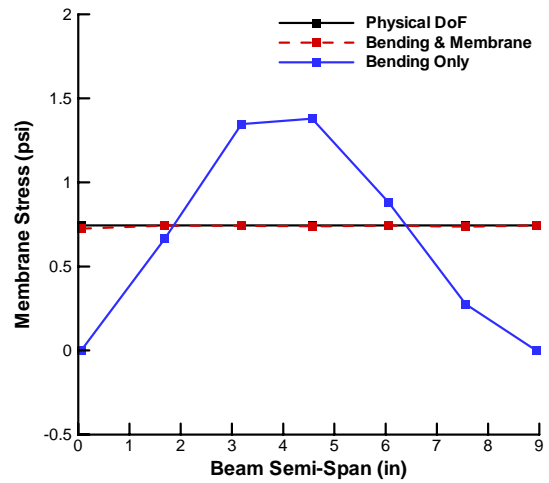

Figure 4: Quasi-static membrane stress along beam under 0.0576 psi pressure load.

A compact measure of the displacement and stress error along the span of the beam, relative to the physical DoF solution, may be found from

$$\% \, Error = \left[\frac{1}{N} \sum_{i=1}^{N} \sqrt{\frac{\left(Physical_i - Reduced \, Order_i \right)^2}{Physical_i^2}} \right] \times 100 \qquad (13)$$

where N is a number of points along the beam span used for the estimation. Figure 5 and Figure 6 present the displacement and stress errors, respectively, computed using results obtained at the seven locations ($N=7$) shown in Figure 1 – Figure 4. It is seen that the bending and membrane basis provides excellent agreement through the entire range of excitation levels studied, and validates both the nonlinear modal stiffness formulation and the implementation. The large error associated with the bending only basis is indicative of the quality of results that may be achieved in the subsequent linear and equivalent linear analyses.
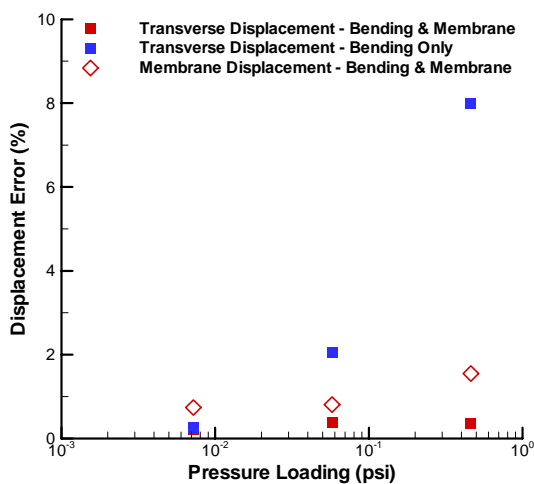

Figure 5: Quasi-static displacement error integrated along the beam semi-span.
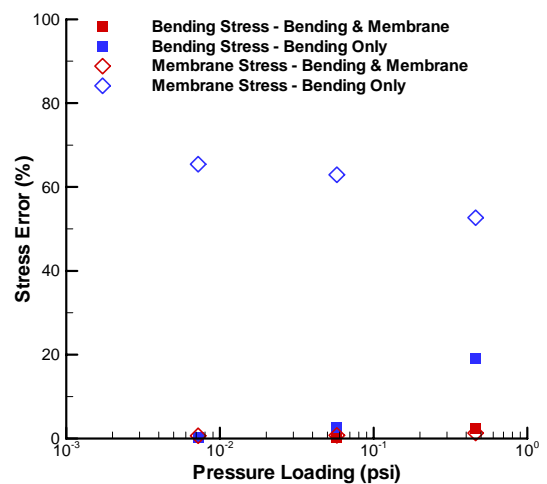

Figure 6: Quasi-static stress error integrated along the beam semi-span.

SOLUTION PROCEDURES

Two solution procedures of differing fidelity and computational burden are considered. The equivalent linearization solution is fast, but accurate only in an RMS sense. The nonlinear modal simulation is accurate in terms of its ability to capture nonlinear spring stiffening and softening, and broadening of the power spectral density. It comes at greater computational expense relative to equivalent linearization, but less relative to simulation in physical DoFs.

Equivalent linearization. An approximate solution to Equation (2) can be achieved by formation of an equivalent linear system:

$$\tilde{M}\ddot{q}(t) + \tilde{C}\dot{q}(t) + \tilde{K}_{eq}q(t) = \tilde{F}(t) \tag{14}$$

where $\tilde{K}_{eq}$ is the modal equivalent linear stiffness matrix given by

$$\tilde{K}_{eq} = \Phi^T K_{eq}\Phi . \tag{15}$$

Using the force-error minimization method of equivalent linearization, the modal equivalent linear stiffness matrix is determined in an iterative approach, as discussed in [7]. For the first iteration, $\tilde{K}_{eq}$ is simply the linear modal stiffness coefficient matrix. For subsequent iterations ($m>1$), the nonlinear stiffness is written as

$$\tilde{K}_{eq}^m = \begin{bmatrix} d_1^1 + \sum_j^L a_{j1}^1 E[q_j] + \sum_{j=1}^L \sum_{k=j}^L b_{jk1}^1 E[q_j q_k] & \cdots & \sum_j^L a_{jL}^1 E[q_j] + \sum_{j=1}^L \sum_{k=j}^L b_{jkL}^1 E[q_j q_k] \\ \vdots & \ddots & \vdots \\ \sum_j^L a_{j1}^L E[q_j] + \sum_{j=1}^L \sum_{k=j}^L b_{jk1}^L E[q_j q_k] & \cdots & d_L^L + \sum_j^L a_{jL}^L E[q_j] + \sum_{j=1}^L \sum_{k=j}^L b_{jkL}^L E[q_j q_k] \end{bmatrix}^{m-1} .$$

Once $\tilde{K}_{eq}$ is known, Equation (14) can be solved in the time domain or frequency domain, with subsequent modal results transformed back to physical coordinates. In this paper, the equivalent linear system is numerically integrated so that response time histories may be obtained.

Nonlinear modal simulation. For the nonlinear modal simulation procedure, the coupled modal nonlinear equations of motion in Equation (2) are numerically integrated using a fourth-order Runge-Kutta method. The resulting modal displacement time histories are transformed back to physical coordinates using the inverse modal transformation.

The equivalent linearization and numerical simulation solutions have been implemented in FORTRAN programs in RANSTEP, and operate independent of the particular finite element program used to generate the modal nonlinear stiffness coefficients.

Stress recovery. Element stress recovery is performed by post-processing the nodal physical DoFs directly within the finite element program. A stress time history is obtained by specifying the physical DoFs for the element(s) of interest at each simulation output time step. As a result, the stresses are identical to those that would have been obtained via a finite element analysis in physical DoFs.

For the equivalent linear analysis, stress time histories are recovered using a linear static analysis procedure with specified nodal displacements obtained from each integration output time step. In MSC.NASTRAN, the linear static solution 101 with multiple subcases is used.

8

In ABAQUS Standard, the *STATIC solution is used. For either finite element program, the stress recovery mesh need only encompass the element or elements of interest, and therefore the process generally has a light computational burden. A nuance of MSC.NASTRAN requires the additional attachment of a dummy element and load to the stress recovery element, in order to calculate the resulting element nodal forces and recover the element stress.

For the nonlinear modal simulation analysis, stress time histories are instead recovered using a nonlinear static analysis procedure. In MSC.NASTRAN, the nonlinear static solution 106 with multiple subcases is used. In ABAQUS, either the Standard analysis (using the *STATIC solution with geometric nonlinearity enabled) or Explicit analysis is used. The ABAQUS Explicit analysis has been found to be significantly faster than the Standard analysis, but requires that the initial conditions additionally be specified in the first analysis step. This is because the Explicit analysis is still being run as if it were a dynamic analysis and not a series of unrelated static cases.

RANDOM RESPONSE

A clamped-clamped beam under a uniformly distributed random pressure loading with a bandwidth of 1500 Hz was chosen to demonstrate the quality of results obtainable via a linear modal solution, equivalent linear solution, nonlinear modal simulation, and numerical simulation in physical DoFs. This structure was selected as it exhibits nonlinear bending-membrane coupling and is sufficiently small in size to perform the numerical simulation in physical DoFs within a reasonable period of time. The analysis of a more practical structure is the subject of reference [8].

The linear modal, equivalent linear and nonlinear modal simulation analyses use the MSC.NASTRAN beam model and properties previously discussed. The linear modal and equivalent linear analyses used the lowest six symmetric bending modes in the modal transformation, while the nonlinear modal simulation used both the lowest six symmetric bending modes and the lowest six anti-symmetric membrane modes. The numerical simulation in physical DoFs was performed using the ABAQUS explicit solution and the beam model previously discussed. Damping was chosen to be sufficiently high so that good comparisons could be made at the peaks of the power spectral density (PSD) function. A level of mass proportional damping was specified corresponding to 2.0% critical damping for the first symmetric bending mode.

Load generation and ensemble averaging. The same loading time history and ensemble averaging was used for all analyses. The loading time histories were generated by summing equal amplitude sine waves, each with random phase, within the specified bandwidth using a discrete inverse Fourier transform. This procedure was identical to that used in previous work [7] by the authors, so further details are omitted for brevity. The loading produced by this method has a Gaussian distribution. A sharp roll-off of the input spectrum practically eliminates excitation of the structure outside the frequency range of interest.

A range of load levels was considered to span the response regime from nearly linear to highly nonlinear. For each load level, ten ensembles of displacement and stress response were generated lasting $2.1384s$ each. The first $0.5s$ of each response record was discarded to remove the initial transient response [7], resulting in response histories of $1.6384s$ in duration. For each simulation, the displacement and stress response was stored at every $50\,\mu s$, giving time records of 32,768 points. A 32,768-point FFT was subsequently used to compute the PSD function.

Results. Displacement and stress results are presented at approximately the ¼-span location to highlight the contribution of the membrane response. Displacement results were obtained at the node located at 4.5-in. from the clamped end. Element stress results were obtained at an adjacent element, with a stress recovery point at 4.4375-in. from the clamped end.

The root-mean-square (RMS) transverse displacement is shown in Figure 7 for a range of loadings. The equivalent linear analysis indicates a nonlinear response. Thus, there is a need to run the more accurate nonlinear modal simulation to obtain stress time histories needed for the fatigue estimate. The best comparison with numerical simulation in physical DoFs is achieved using the nonlinear modal simulation, which slightly over-predicts the response. Good agreement is also achieved, however, with the equivalent linear analysis. Note that the inclusion of six additional anti-symmetric membrane modes (not shown) in either the linear modal or equivalent linear analyses does not significantly change the quality of the comparison. This is due to the lack of linear bending-membrane coupling for this problem. The RMS membrane displacement is shown in Figure 8. Compared to the physical DoF results, the level of agreement achieved using the nonlinear modal simulation is very good. Since the membrane displacement only manifests itself via nonlinear bending-membrane coupling for this problem, the linear modal and equivalent linear analysis are incapable of generating any membrane displacement component for a basis consisting of only bending modes.
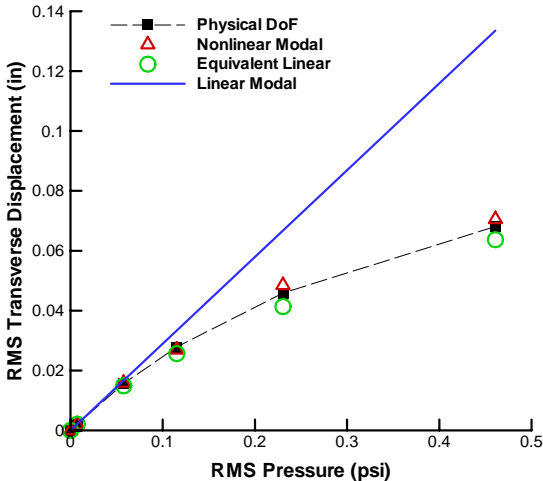

Figure 7: RMS transverse displacement as a function of random pressure load.
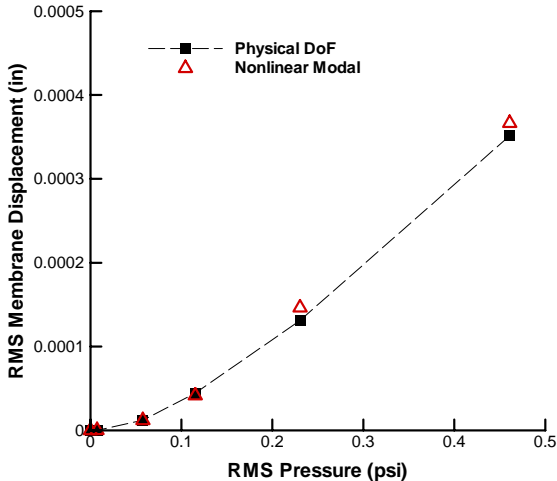
Figure 8: RMS membrane displacement as a function of random pressure load.

The transverse displacement PSD for the highest RMS pressure of 0.4608 psi (164 dB) is shown in Figure 9. For this level, the response is highly nonlinear and exhibits nonlinear spring hardening, seen by a shift in the peak response to higher frequencies relative to the linear analysis and peak broadening. Very good agreement between the nonlinear modal and physical DoFs solution is seen across the frequency range. The equivalent linear analysis, which was seen to agree fairly well in an RMS sense, is significantly different from the physical DoFs solution, highlighting the need for a more accurate response calculation. The magnitude of the peak response is different, the shifting of peaks to higher frequency is exaggerated, and it lacks the peak broadening characteristic. The linear modal response, as expected, captures none of the essential characteristics. The corresponding membrane displacement PSD, shown in Figure 10, indicates that the nonlinear modal simulation captures the essential features of period doubling, with greater differences observed at the higher

frequencies. Again, the linear modal and equivalent linear analyses are incapable of predicting the membrane displacement.
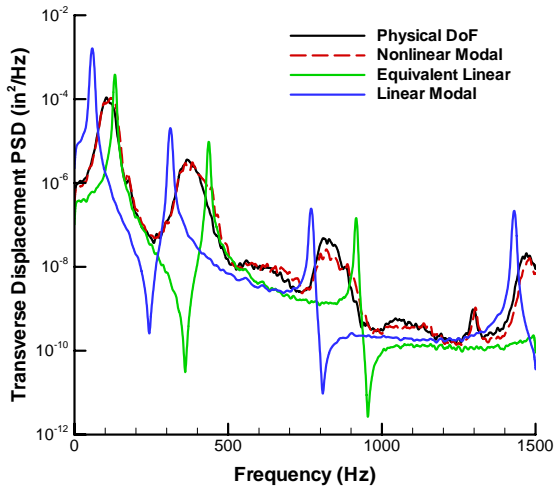

Figure 9: Transverse displacement PSD for a 164 dB random pressure loading.
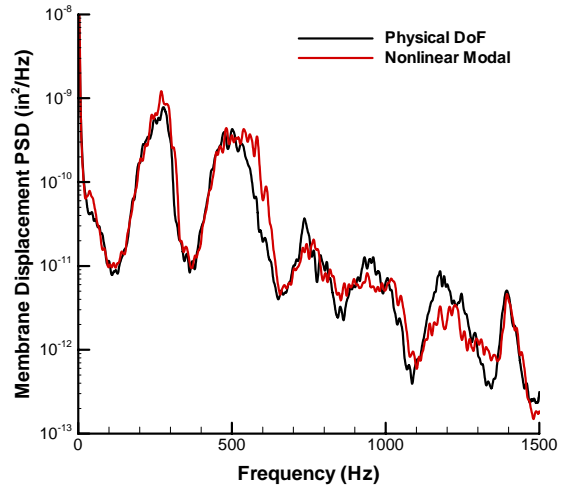

Figure 10: Membrane displacement PSD for a 164 dB random pressure loading.

Figure 11 shows the normal stress PSD on the beam surface corresponding to the highest loading of 164 dB. The nonlinear modal simulation agrees very well with the solution in physical DoFs. Note the significant zero frequency component in both the nonlinear modal simulation and physical DoFs analyses. This is due to the membrane stress component, which oscillates between zero and some positive value. For the physical and nonlinear modal simulations, the membrane stress skews the probability distribution function (PDF) to the positive stress range, as shown in Figure 12. Here the PDF has been normalized by the standard deviation. The equivalent linear and linear modal stress PSDs bear little resemblance to the solution in physical DoFs. Further, these analyses are unable to predict the membrane stress. Consequently, the zero frequency component is small for the equivalent linear and linear modal solutions and their PDFs are nearly Gaussian, with zero skewness.
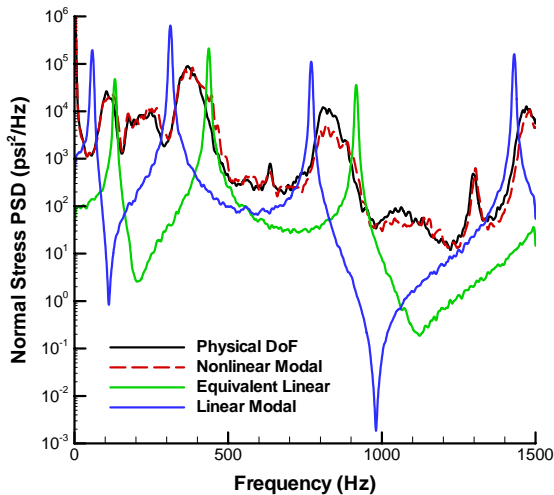

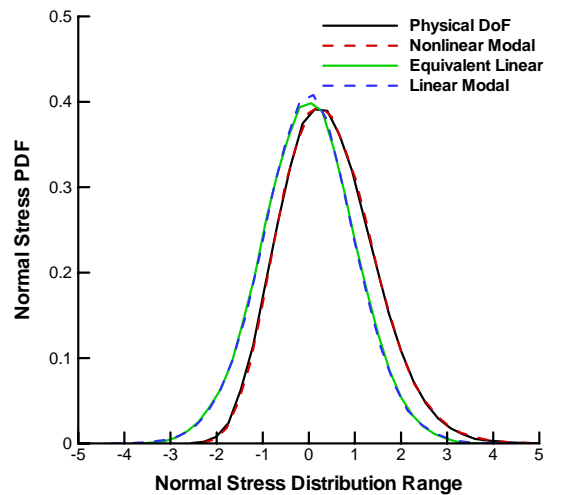*Figure 11: Normal stress PSD for a 164 dB random pressure loading.*

Figure 12: Normalized normal stress PDF for a 164 dB random pressure loading.

To recap, the equivalent linear analysis was seen to be a good indicator of nonlinear response through observation of the RMS transverse displacement. As expected, it was not sufficient to adequately compute the membrane behavior, the displacement PSD, and stress PSD.

Hence, a more accurate means of computing these quantities is required. The nonlinear modal simulation was able to meet that need, provided a sufficient modal basis is used. Therefore, in the following fatigue analysis, results from the nonlinear modal simulation are considered as the only alternative to the results from the simulation in physical DoFs.

FATIGUE ANALYSIS

For a constant amplitude, zero-mean stress response, the stress-life (*S-N*) curve relates the cycles to failure, N_f, to the fully reversed alternating stress, σ_{ar}, via the power law:

$$\sigma_{ar} = A N_f^b \tag{16}$$

where $A = \sigma_f' 2^b$, and σ_f' and b are material properties determined from tests performed under zero-mean stress. The fatigue life can then be determined from

$$N_f = \left(\frac{\sigma_{ar}}{A} \right)^{1/b} . \tag{17}$$

For conditions having a non-zero mean stress, a number of models are available, see [9]. In this paper, we consider the Walker model, which expresses the alternating stress as:

$$\sigma_{ar} = \sigma_{max} \left(\frac{1-R}{2} \right)^\gamma , \qquad \text{where } R = \frac{\sigma_{min}}{\sigma_{max}} \tag{18}$$

and the number of cycles to failure as:

$$N_{fw} = \left[\sigma_{max} \left(\frac{1-R}{2} \right)^\gamma \frac{1}{A_w} \right]^{1/b_w} , \qquad \text{where } A_w = \sigma_{fw}' 2^{b_w} . \tag{19}$$

In the above, σ_{fw}', b_w γ are material properties determined from tests performed under a range of stress ratios R. For fully reversed loadings, $R = -1$ and $\sigma_{ar} = \sigma_{max}$.

The Palmgren-Miner linear cumulative damage rule [10] is typically used for variable amplitude loading and assumes that the damage, *D,* caused by stress cycles at one stress level can be calculated and added to damage caused by stress cycles in another stress level, or

$$D = \sum_i \frac{N_i}{\left(N_f \right)_i} \tag{20}$$

where N_i are the number of cycles at stress level σ_i, and $\left(N_f \right)_i$ are the number of cycles to failure at stress level σ_i.

Random fatigue. For random response, it is convenient to recast Equation (20) in the form

$$E[D] = E[P] T \sum_{-\infty}^{\infty} \sum_{-\infty}^{\infty} \frac{p\left(\sigma_{min}, \sigma_{max} \right) \Delta\sigma_{min} \Delta\sigma_{max}}{N_f \left(\sigma_{min}, \sigma_{max} \right)} \tag{21}$$

where $E[P]$ are the number of peaks per second, T is the lifetime, $p(\sigma_{min}, \sigma_{max})$ is the joint PDF of stress minimum and maximum values, and $\Delta\sigma_{min}$ and $\Delta\sigma_{max}$ are the PDF bin widths.

The dependency of N_f on $\sigma_{\min}$ and $\sigma_{\max}$ is determined by the particular model used, e.g. zero-mean, Walker, etc.

Rainflow analysis. It was shown in [11] that $p(\sigma_{\min}, \sigma_{\max})$ can be estimated from the rainflow matrix (RFM)

$$\frac{1}{N_{RF}}\sum_{-\infty}^{\infty}\sum_{-\infty}^{\infty}RFM\left(\sigma_{\min},\sigma_{\max}\right)=\sum_{-\infty}^{\infty}\sum_{-\infty}^{\infty}p\left(\sigma_{\min},\sigma_{\max}\right)\Delta\sigma_{\min}\Delta\sigma_{\max} \tag{22}$$

where N_{RF} are the number of rainflow cycles. The RFM is a two-dimensional histogram of rainflow ranges. In this paper, the RFM was obtained using the WAFO Matlab toolbox for analysis of random waves and loads [12]. For a finite record of duration $T_{\max}$, $E[P]=N_{RF}/T_{\max}$. Substitution of Equation (22) into (21) then yields

$$E\left[D\right]=\frac{T}{T_{\max}}\sum_{-\infty}^{\infty}\sum_{-\infty}^{\infty}\frac{RFM(\sigma_{\min},\sigma_{\max})}{N_f(\sigma_{\min},\sigma_{\max})}=\frac{T}{T_{\max}}\sum_{-\infty}^{\infty}\sum_{-\infty}^{\infty}RFD(\sigma_{\min},\sigma_{\max})$$

where $RFD(\sigma_{\min},\sigma_{\max})$ is the two-dimensional rainflow damage matrix. Failure occurs when $E\left[D\right]=1$, giving the estimated fatigue life T as

$$T=\ T_{\max}\left/\sum_{-\infty}^{\infty}\sum_{-\infty}^{\infty}\frac{RFM(\sigma_{\min},\sigma_{\max})}{N_f(\sigma_{\min},\sigma_{\max})}\right. \tag{23}$$

Note that since damage is calculated for each bin of the RFM, the quantities in Equation (18) vary with each cycle.

Fatigue results. Fatigue life estimates were made at two locations on the beam previously considered. A position near the clamped end (0.0625-in. from the clamped end) was selected because it exhibits the highest stress and has the shortest fatigue life. A second position near the ¼-span (4.4375-in. from the clamped end) was selected to show the effect of a significant membrane component on the fatigue life prediction. At each loading level, ten normal stress history records were joined together to form an overall record length of $T_{\max}$ = 16.384s. *S-N* properties for 2024-T3 aluminum were used [9], with σ'_f = 1602 and b = -0.154 for the zero mean case, and σ'_{fw} =1772, b_w = -0.163, and γ = 0.460 for the Walker model, when the stress is expressed in units of MPa. For the Walker fatigue estimate, damage was not accumulated for cycles with $R<-2$ as the *S-N* data is not considered valid in this range.

It is useful to first investigate the rainflow matrix. The RFM for the clamped end at the 164 dB loading is shown in Figure 13. The RFM in the upper left domain was generated from the stress time history obtained from the simulation in physical DoFs. Superimposed in the lower right domain is the RFM obtained from the nonlinear modal simulation. If the two were identical, they would form the reverse mirror image of each other. Recall that the membrane stress component accounts for the zero frequency component and hence for the skewness in the normal stress response. Even though the normal stress is dominated by the bending component at this location, the membrane stress still skews the RFC matrices, as evidenced in data from both for the physical and nonlinear modal simulations. The solid diagonal line in Figure 13 indicates the fully-reversed ($R=-1$) rainflow cycles.

Fatigue life estimates at the clamped end are presented in Table 1. Estimates were made using the zero-mean and Walker models. The estimates are expressed in ranges and were obtained by scaling the stress time histories up and down by 10%. This was done in an effort to reflect the sensitivity of the life prediction to variability in the stress prediction. Also shown are the stress standard deviation and mean. Previous work indicated that zero-mean models produce non-conservative fatigue estimates relative to non-zero mean models for tensile mean stress conditions [11, 13]. Estimates made using data from both physical and nonlinear modal simulations confirm this finding. It is interesting to note, however, that as the mean stress component increases from roughly 5% of the standard deviation at the 146 dB level, to roughly 14% at the 164 dB level, the difference between zero-mean and non-zero mean life estimates is reduced from about a factor of 3 (153 vs 53 years, for example), to less than a factor of 2 (3.05 vs 1.68 hours). In general, life estimates made using nonlinear modal simulation stress time histories compare favorably, though somewhat non-conservatively, with those made using physical simulation stress time histories. To understand why, it is helpful to look at the rainflow damage matrix. Figure 14 shows the Walker rainflow damage matrices corresponding to Figure 13. The RFD in the upper left domain was generated from the physical simulation RFM, while the RFD superimposed in the lower right domain was generated from the nonlinear modal simulation RFM. More damage occurs at the high stress amplitudes for the physical DoFs solution than at the high stress amplitudes for the nonlinear modal simulation. Consequently, life estimates made from physical simulation data are lower than those obtained using nonlinear modal data.
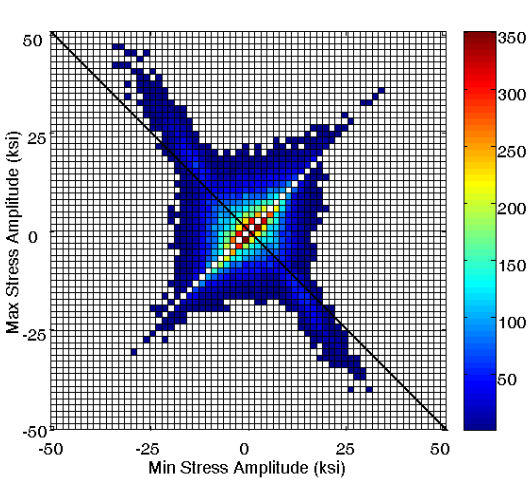

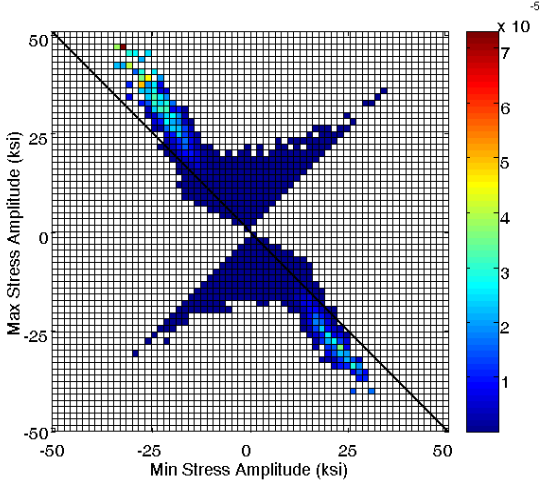*Figure 13: Rainflow matrices at clamped end for 164 dB loading.*

Figure 14: Walker rainflow damage matrices at clamped end for 164 dB loading.

Table 2 presents fatigue life estimates at the ¼-span location, where the membrane stress is more significant. While this location will not dictate the failure of the beam structure, it is nevertheless interesting to note that fatigue life estimates from the nonlinear modal simulation agree very well with those obtained from the physical DoFs simulation.

In summary, both zero-mean and Walker fatigue life estimates obtained using nonlinear modal simulation data compare quite favorably with estimates made using physical simulation data, irrespective of the location, because the stress response from which the estimate is derived is in close agreement.

Table 1: Stress standard deviation, mean, and fatigue life estimates
at the clamped end for a range of loadings.

OASPL (dB)	Stress Std. Dev. / Mean (psi)		Zero Mean Fatigue Life Estimate		Walker Fatigue Life Estimate	
	Physical DoFs	Nonlinear Modal	Physical DoFs	Nonlinear Modal	Physical DoFs	Nonlinear Modal
146	1379 / 69	1332 / 68	153–563 yr	215–791 yr	53.0–181 yr	73.8–253 yr
152	2685 / 210	2466 / 194	1.65–6.08 yr	3.07–11.3 yr	0.63–2.17 yr	1.24–4.28 yr
164	8751 / 1211	8235 / 1170	3.05–11.2 hr	6.17–22.7 hr	1.68–5.74 hr	3.49–12.0 hr

Table 2: Stress standard deviation, mean, and fatigue life estimates
at the ¼-span for a range of loadings.

OASPL (dB)	Stress Std. Dev. / Mean (psi)		Zero Mean Fatigue Life Estimate		Walker Fatigue Life Estimate	
	Physical DoFs	Nonlinear Modal	Physical DoFs	Nonlinear Modal	Physical DoFs	Nonlinear Modal
152	868 / 215	815 / 198	1823–6711 yr	2796-10289 yr	387–1324 yr	554–1897 yr
164	2986 / 1224	2951 / 1269	0.61–2.24 yr	0.72–2.64 yr	0.13–0.47 yr	0.15–0.50 yr

CONCLUDING REMARKS

Two reduced-order analysis methods, equivalent linearization and nonlinear modal simulation, have been presented. These methods have been implemented in the program RANSTEP, which utilize the finite element programs MSC.NASTRAN and ABAQUS to evaluate the nonlinear modal stiffness and perform stress recovery. The nonlinear modal stiffness formulation and implementation has been shown to recover the solution in physical degrees-of-freedom when a suitable modal basis is used.

The two analysis methods were shown to offer complementary capabilities for the analysis of high cycle fatigue. The equivalent linearization analysis was shown to be an effective screening tool to determine if a higher fidelity nonlinear analysis is required. If no significant nonlinearity is indicated, then fatigue estimates based on the customary linear analysis should be adequate. Similarly, if significant nonlinearity is indicated, a nonlinear modal simulation may be used to efficiently compute the fatigue life. Since the accuracy of either reduced-order method is determined largely by the modal basis used, confidence in the results obtained must be established through comparison with either experimental data or other representative analyses. In the present work, displacement response, stress response, and fatigue life predictions made using nonlinear modal simulation results compared favorably with those obtained from the solution in physical DoFs.

REFERENCES

1. Spottswood, S.M., Wolfe, H.F., and Brown, D.L., "The effects of record length on determining the cumulative damage of a ceramic matrix composite beam.," *Structural Dynamics: Recent Advances, Proceedings of the 7th International Conference*, Vol. 2, pp. 785-799, Southampton, UK, 2000.
2. Muravyov, A.A. and Rizzi, S.A., "Determination of nonlinear stiffness with application to random vibration of geometrically nonlinear structures," *Computers and Structures*, Vol. 81, No. 15, pp. 1513-1523, 2003.
3. Mignolet, M.P., Radu, A.G., and Gao, X., "Validation of reduced order modeling for the prediction of the response and fatigue life of panels subjected to thermo-acoustic effects," *Structural Dynamics: Recent Advances, Proceedings of the 8th International Conference*, Southampton, UK, 2003.
4. Rizzi, S.A., "On the use of equivalent linearization for high-cycle fatigue analysis of geometrically nonlinear structures," *Structural Dynamics: Recent Advances, Proceedings of the 8th International Conference*, Southampton, UK, 2003.
5. Rizzi, S.A. and Przekop, A., "The effect of basis selection on static and random response prediction using nonlinear modal simulation," NASA TP-2005-213943, December 2005.
6. Przekop, A. and Rizzi, S.A., "Nonlinear reduced order random response analysis of structures with shallow curvature," *To appear in the AIAA Journal*, 2006.
7. Rizzi, S.A. and Muravyov, A.A., "Comparison of nonlinear random response using equivalent linearization and numerical simulation," *Structural Dynamics: Recent Advances, Proceedings of the 7th International Conference*, Vol. 2, pp. 833-846, Southampton, UK, 2000.
8. Przekop, A., Rizzi, S.A., and Groen, D.S., "Nonlinear acoustic response of an aircraft fuselage sidewall structure by a reduced-order analysis," *Structural Dynamics: Recent Advances, Proceedings of the 9th International Conference*, Southampton, UK, 2006.
9. Dowling, N.E., "Mean stress effects in stress-life and strain-life fatigue," *Fatigue 2004: Second SAE Brasil Conference on Fatigue*, SAE 2004-01-2227, São Paulo, Brasil, June, 2004.
10. Miner, M.A., "Cumulative damage in fatigue," *Trans. ASME, Journal of Applied Mechanics*, Vol. 67, pp. A159-A164, 1945.
11. Sweitzer, K.A. and Ferguson, N.S., "Mean stress effects on random fatigue of nonlinear structures," *XII International Congress on Sound and Vibration*, Lisbon, Portugal, July, 2005.
12. "WAFO - A Matlab toolbox for analysis of random waves and loads," Version 2.1.1, The WAFO Group, Lund Institute of Technology, Lund University, 2005.
13. Kihl, D.P. and Sarkani, S., "Mean stress effects in fatigue of welded steel joints," *Probabilistic Engineering Mechanics*, Vol. 14, pp. 97-104, 1999.